Journal of JSEM, Vol.11, Special Issue (2011) SS221-SS226

Impact Tensile Properties of Structural Sintered Steels

Kinya KAWASE[1, 2], Yuji TANABE[2, 3], Tomoyuki YAMAZAWA[2] and Hiroaki SUZAWA[2]

[1] Diamet Corporation, Niigata 950-8640, Japan
[2] Graduate School of Science and Technology, Niigata University, Niigata 950-2181, Japan
[3] Education Centre for Engineering and Technology, Niigata University, Niigata 950-2181, Japan

(*Received 10 January 2011; received in revised form 22 April 2011; accepted 5 June 2011*)

Abstract
This study deals with the mechanical properties of two kinds of structural sintered steels under a wide range of strain rate between 10^{-4} and $10^{3}s^{-1}$. The split-Hopkinson pressure bar (SHPB) technique was used for dynamic tensile tests at the strain rates greater than $10^{2}s^{-1}$. The stress-strain relations were experimentally determined, and the tensile strength has been mainly discussed with respect to strain rate and relative density.

Key words
Structural Sintered Steels, Dynamic Tensile Test, Split-Hopkinson Pressure Bar Technique, Tensile Strength, Relative Density, Strain Rate Dependent Behaviour

1. Introduction

Structural sintered steels are usually used at their relative density [1] of approximately 90%, and their tensile strengths are almost equivalent to pore free wrought steels [2]. For instance, conventional Fe-2Cu-0.5C (in mass%) steel has a static tensile strength of around 400MPa and high strength Fe-4Ni-1.5Cu-0.5Mo-0.5C steel shows that of around 600MPa. However, these sintered steels obviously show inferior characteristics in toughness to the ingot steels. Due to this, the Charpy tests on them have been performed with notchless specimens instead of notched specimens usually used for the other materials [3]. Furthermore, the notchless sintered steel specimens showed extremely low impact toughness of around between 10 and 20J/cm^2 while the U-notched ingot steel specimens showed that around 50 to 100J/cm^2 [2]. Thus, the sintered steels subjected to dynamic or impact loading are very brittle, and therefore a number of studies concerning their impact characteristics mainly obtained from the Charpy tests have been reported in Ref. [4-12] so far. However, the Charpy impact toughness can not be directly used as fundamental data for machine design and the toughness of notchless specimen can not be compared with that of notched specimens of wrought materials as well. The economically advantageous sintered steels should be consequently kicked out of the list of the candidate materials for machine components possibly subjected to impact loading. Therefore, it should be industrially very useful to obtain the dynamic tensile properties of the sintered steels as fundamental but the most important characteristic among the mechanical properties especially under dynamic loading, or high strain rate. However, the limited number of studies on the dynamic tensile properties of the sintered steels and the other steels made through powder metallurgy has been done. Nahme et al. investigated the dynamic mechanical properties of TiB_2 particle-reinforced stainless steels in conjunction with their microstructures, and observed the significant increases in both static and dynamic tensile strengths due to the particle reinforcement [13]. Lee et al. discussed the impact tensile behaviours of sintered stainless steels and Fe-2Ni alloy, and revealed their tensile strengths increased at higher strain rates [14]-[16].

As mentioned above, there have been only a few previous studies concerning the tensile properties of the sintered steels under high strain rates, however, no sufficient data has been obtained yet to well understand their fracture manners at high strain rates. In particular, although the sintered steels, namely Fe-2Cu-0.5C and Fe-4Ni-1.5Cu-0.5Mo-0.5C have been generally and widely used for many sorts of mechanical parts such as oil pump rotors, gears, cams, pulleys and so on, both the steels have not been well treated as target materials for investigation so far. Cu is widely used next to C as an alloying element in the structural sintered steels since Cu is easy to be deoxidised and very effective to make the sintered steels stronger [17]. Diffusion alloyed steel, namely Fe-Ni-Cu-Mo-C made from the mixture of the powder of Fe partially alloyed with the powders of Ni, Cu, and Mo and the powder of C, has been used as material for the components which require high strength and good precise formability [17]. It is, therefore, very important for understanding the real aspects of their fracture mechanics as well as for the extent of applicability through the improvement of their mechanical properties to assess and analyse the impact tensile properties.

This study deals with the effect of strain rate on the mechanical properties, namely stress-strain response and tensile strength of the two conventional sintered steels mentioned above with respect to their relative density. To this end, both quasi-static and impact tensile tests on them have been performed.

2. Materials and Methods

2.1 Materials

Materials used in this study were two kinds of sintered steels, namely Fe-2Cu-0.5C (Steel M) and Fe-4Ni-1.5Cu-0.5Mo-0.5C (Steel D) steels. Both the steels were offered by the manufacturer (Diamet Corp., Japan) and made in accordance with the standard powder compaction process briefly described as below.

The Steel M was made from the raw powders of Fe, Cu and C and the Steel D from those of partially alloyed Fe-4Ni-1.5Cu-0.5Mo and C. The raw powders of each steel were first mixed together at a given mixture ratio for each steel, and then the powder compaction process was applied

to each mixture so as to get the rectangular rods of 60×10×10mm^3 and 80×10×10mm^3 with the relative densities of approximately 85, 90 and 95%. The compacting pressures of 420 and 620MPa were applied to the mixture at room temperature to achieve the relative densities of 85 and 90%, respectively, while the compacting pressure of 710MPa at 120°C was chosen to get the rods with the relative density of 95%. All the compacted rods were sintered in endothermic gas at 1120°C for 1.2ks. After being sintered, the rods were machined into dumbbell shaped tensile specimens. The quasi-static tensile specimens with gauge section 26mm long and 4.5mm in diameter [18] were machined from the rods of 80×10×10mm^3, while the specimens with gauge section 4mm long and 4mm in diameter for impact tensile tests (Fig.1) were machined from those of 60×10×10mm^3.

The physical and static mechanical properties of the Steel M and D are listed in Table 1. In this table, material symbols are appeared as capital letters (the same symbols of the investigated steels) followed by the values of the relative density, respectively.

In order to recognise the size effect of specimen on tensile strength, the specimens shown in Fig.1 of the Steel M and D with the relative density of 85% were subjected to quasi-static test. Tensile strengths of the D-85 and M-85 with the specimens in Fig.1 were 498 and 317MPa, respectively. It was confirmed that they were almost same as the tensile strength with ISO standard specimens shown in Table 1.

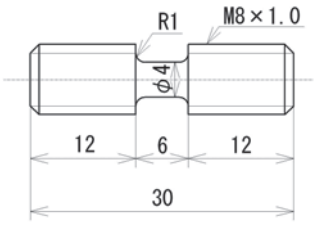

Fig.1 Specimen geometry and dimensions for tensile SHPB experiment

Table 1 The physical and static mechanical properties of the Steel M and D

Material	Density ρ [Mg/m^3]	Relative density [%]	$\sigma_{0.2}$ [MPa]	σ_B [MPa]	Elongation ψ [%]	Young's modulus [GPa]
D-85	6.77	86	313	515±2	1.2	113±6
D-90	7.11	91	352	643±8	2.4	140±19
D-95	7.39	94	371	723±8	3.3	162±6
M-85	6.67	86	239	318±2	0.6	108±15
M-90	7.01	90	287	401±10	0.9	134±5
M-95	7.31	94	313	438±6	1.4	156±18

2.2 Experimental methods

Quasi-static tensile tests at low strain rates of approximately 7×10^{-4} s^{-1} were performed using an Instron-type materials testing machine with an attachment of extensometer directly to the gauge section of the specimen.

Impact tensile tests at high strain rates between 4×10^{1} and 8×10^{2}s^{-1} were performed using the SHPB apparatus (Fig.2). The SHPB apparatus consists basically of an air gun, a striker bar, two Hopkinson pressure bars, designated "Bar No.1" and "Bar No.2", respectively, and recording equipments. These three bars are made of 20mm diameter bearing steel rods. In this particular type of the tensile SHPB apparatus originally developed by Nicholas [19], after the specimen was screwed into the Bars No.1 and No.2 as shown in Fig.3, a split-collar, made of the same material as the Hopkinson bars, with outer and inner diameters of 20mm and 8mm, respectively, was placed between the pressure bars over the gauge length of the specimen and properly tightened by twisting one of the bars. The ratio of the cross-sectional area of the collar to that of the Bars No.1 and No.2 is 0.84:1, whereas the ratio of the area of the collar to the net cross-sectional area of the parallel part of the specimen is 21:1. A compressive strain pulse generated by an impingement of the striker bar on the Bar No.1 travels through the composite cross section of the collar and specimen without serious compression to the specimen (simple calculation based on the area ratio mentioned above expects the pre-compression with the magnitude of approximately 10% of the incident load to the specimen) and transmits into the Bar No.2. When the compressive strain pulse reaches the free end of the Bar No.2, it reflects and propagates backward as a tensile strain pulse (ε_t). The tensile pulse, on reaching the specimen-Bar No.2 interface, is partially transmitted through the specimen (ε_t) and partially reflected back into the Bar No.2 (ε_r). Note that the collar, in which the most of compressive pulse passed through, is

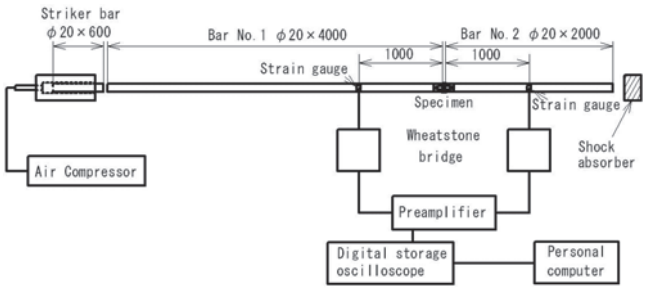

Fig.2 Schematic of tensile SHPB apparatus

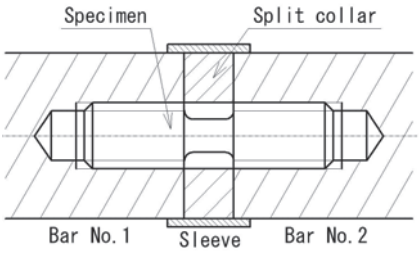

Fig.3 Detail of attachment of specimen into SHPB apparatus

unable to support any tensile loads because it is not fastened to the bars. Consequently, the entire tensile loading of the specimen can be achieved if we use the tensile strain pulse as an incident strain one. That is, after the tensile strain is reflected from the free end of the Bar No.2 and starts to propagate backward along the bar, the experimental apparatus becomes identical to the compressive SHPB apparatus widely used in the previous studies except for the change in sign of the loading pulse and the use of a threaded joint to attach the specimen in place of a cylindrical compression specimen [19]. In the apparatus, signals of the incident, reflected and transmitted strain waves were detected by two sets of foil strain gauges with a gauge length of 1mm (Kyowa, Type KFG-1N-120-C1-11L1M2R) glued on the Bars No.1 and No.2, respectively, and stored in a digital storage oscilloscope (Recroy, Model Wave Pro 715ZI) with a sampling frequency of 10MHz. Typical oscilloscope records for the tensile SHPB tests on the Steel M are shown in Fig.4. Nominal strain rate $\dot{e}$, strain e and stress s in the specimen are calculated by the Eqs. (1), (2) and (3), respectively:

$$\dot{e}(t) = \frac{C_0}{l}\{\varepsilon_i(t) - \varepsilon_r(t) - \varepsilon_t(t)\} \tag{1}$$

$$e(t) = \frac{C_0}{l}\int_0^t \{\varepsilon_i(t) - \varepsilon_r(t) - \varepsilon_t(t)\}dt \tag{2}$$

$$s(t) = \frac{AE}{2A_s}\{\varepsilon_i(t) + \varepsilon_r(t) + \varepsilon_t(t)\} \tag{3}$$

The force at the Bar No.2/specimen interface P_1 and that at the specimen/Bar No.1 interface P_2 are given as:

$$P_1(t) = AE\{\varepsilon_i(t) + \varepsilon_r(t)\},\ P_2(t) = AE\varepsilon_t(t) \tag{4}$$

If the forces at the both interfaces are equal, that is, P_1=P_2, or $\varepsilon_i(t) + \varepsilon_r(t) = \varepsilon_t(t)$, Eqs. (1), (2) and (3) can be simplified:

$$\dot{e}(t) = \frac{2C_0}{l}\{\varepsilon_i(t) - \varepsilon_t(t)\} \tag{5}$$

$$e(t) = \frac{2C_0}{l}\int_0^t \{\varepsilon_i(t) - \varepsilon_t(t)\}dt \tag{6}$$

$$s(t) = \frac{AE}{A_s}\varepsilon_t(t) \tag{7}$$

True strain rate $\dot{\varepsilon}$, strain ε and stress σ are also calculated by Eqs. (8), (9) and (10), respectively:

$$\dot{\varepsilon} = \frac{\dot{e}}{1+e} \tag{8}$$

$$\varepsilon = \ln(1+e) \tag{9}$$

$$\sigma = s(1+e) \tag{10}$$

In this study, the true stress-true strain responses were obtained using the equations from (5) to (10). The discrepancy between the true stress by Eq.(3) and that by Eq.(7) was confirmed to be within 5%, that is, Eq.(7) gave us the underestimated values of the true stress comparing with Eq.(3). The sintered steels essentially show brittle fracture manner, and so we have decided to use Eq. (7) for the determination of their tensile strengths from the perspective of safe design. Such evaluation could have no effect on any conclusion of the present study.

All tensile tests mentioned above were performed in air and at room temperature of 20°C, and fracture surfaces of some specimens of the Steel M and D with different relative density after tensile testing were observed using a scanning electron microscope (SEM). The SEM micrographs of fracture surfaces were subjected to image analysis to obtain the area ratio according to fracture pattern, of which the ratio to the total fracture area was calculated as the area ratio.

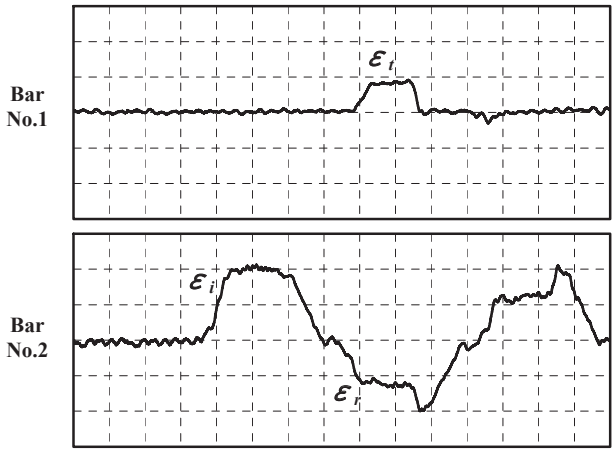

Fig.4 Typical oscilloscope records for tensile SHPB test on the Steel M

3. Results and Discussion

The typical true stress-strain responses of the Steel M and D with the relative density of 95% under various strain rates in this study are shown in Fig. 5. Similar results to Fig.5 were obtained for the other steels independently of strain rate and relative density without any significant difference in Young's modulus. The maximum value of the true stress was determined as the tensile strength, and discussed in this study.

Figure 6 shows the strain rate dependence of the tensile strength for both the Steel D and M. Within the range of strain rate between 4×10^1 and $8\times10^2 s^{-1}$ no clear effect of strain rate on the tensile strength of both the steels was found independently of relative density. However, both the steels appeared to show large tensile strengths under such

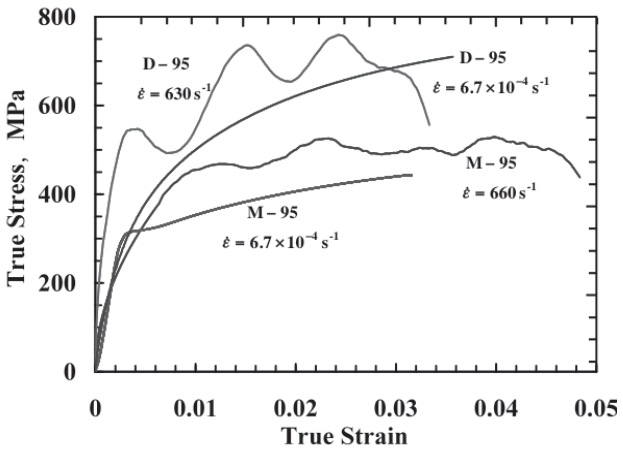

Fig.5 Typical stress-strain curves for the Steel M and D under various strain rates

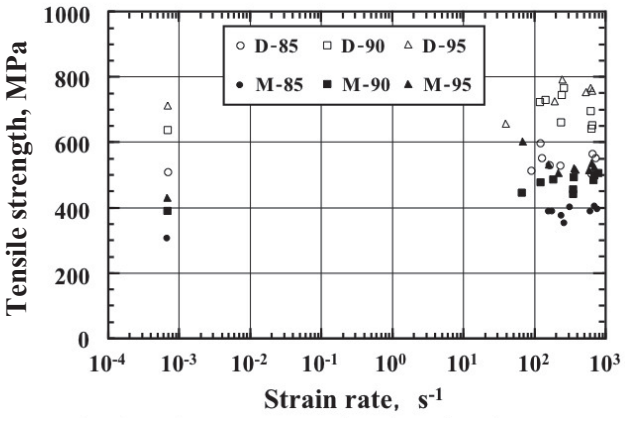

Fig.6 Tensile strength as a function of strain rate

high strain rates compared to those under low strain rate independently of relative density. That is, the difference between quasi-static and impact tensile strengths was small.

Figure 7 shows the tensile strengths of the Steel D and M plotted against relative density. The Steel D clearly showed larger tensile strengths than the Steel M independently of strain rate and relative density. The tensile strength increased with increasing relative density in both the steels independently of strain rate.

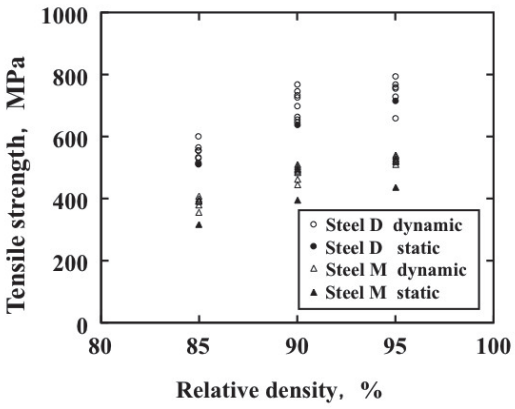

Fig.7 Tensile strength plotted against relative density

Figures 8 and 9 show the SEM micrographs of the fracture surfaces of quasi-static and impact tensile specimens for the Steel M and D with the relative density of 85% and 95%, respectively. And, Tables 2 and 3 show area ratio of fracture patterns of fracture surfaces for the Steel D and M. The Steel M with the relative density of 85% and 90% showed intergranular fracture at prior powder particle boundaries in both the static and impact fracture surfaces, while the transgranular or cleavage fracture in some prior powder particles was observed in the

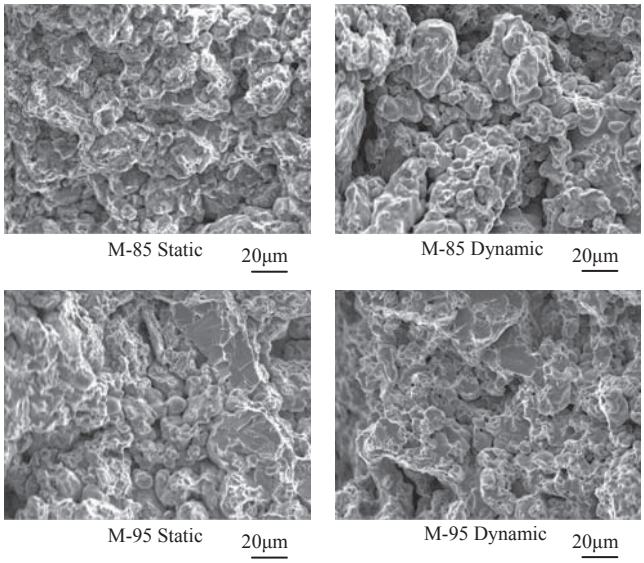

Fig.8 SEM micrographs of the fracture surfaces for the Steel M with the relative density of 85% and 95%

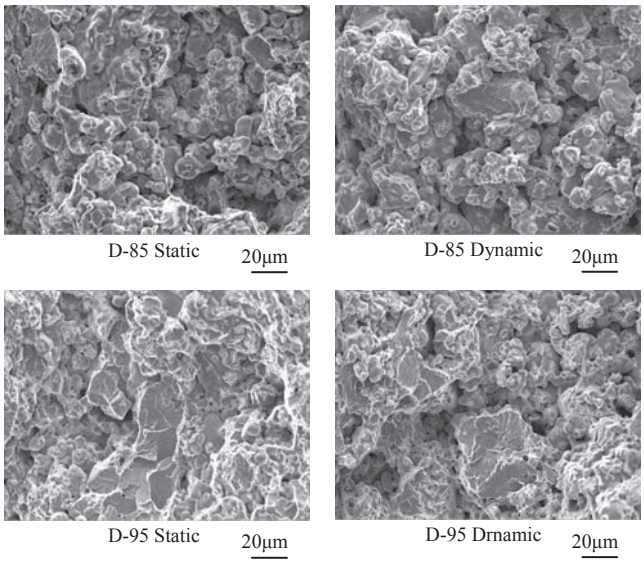

Fig.9 SEM micrographs of the fracture surfaces for the Steel D with the relative density of 85% and 95%

Table 2 Area ratio of fracture patterns of fracture surfaces for the Steel D (area %)

Tensile test		Static			Dynamic		
Material		D-85	D-90	D-95	D-85	D-90	D-95
Fracture pattern	Intergranular	20	21	17	16	18	17
	Transganular	2	5	14	2	4	12
	Non-transformative	78	74	69	82	78	71

Table 3 Area ratio of fracture patterns of fracture surfaces for the Steel M (area %)

Tensile test		Static			Dynamic		
Material		M-85	M-90	M-95	M-85	M-90	M-95
Fracture pattern	Intergranular	20	20	18	18	19	23
	Transganular	0	0	2	0	0	2
	Non-transformative	80	80	80	82	81	75

Steel M with the relative density of 95%. This suggests that the key factor to increasing the tensile strength is thought to be diffusion bonding between the powder particles of Fe. Therefore, larger relative density increases the contact surface area between the powder particles of Fe, which results in the increase of the tensile strength. On the other hand, the Steel M showed the transgranular or cleavage fracture in some prior powder particles even with the lowest relative density. With increasing relative density, area ratio of transgranular or cleavage fracture increased. The effect of density on the tensile strength of the Steel D is considered to be the same as that of the Steel M.

Figure 10 shows the microstructures of the Steel D and the Steel M. From the figure, it can be seen that the Ni rich layer is formed at the contact surface between the Fe particles during the sintering process in the Steel D. Larger area ratio of intergranular fracture of the Steel D comparing with that of the Steel M indicates that the Ni rich layer contributes to enhance adhesive strength of the Fe particles, which is considered to contribute higher tensile strength of the Steel D than that of the Steel M. No clear different aspects in fracture manner between quasi-static and impact tension was recognised in both the Steel M and D. From Tables 2 and 3, it can be found that the majority of fracture surfaces is non-transformative area, which consists of non-transformative prior particle boundaries and pores, in all the conditions. This indicates that the fracture mode of the whole material is brittle, from which it is supposed that the effect of strain rate on tensile strength is small.

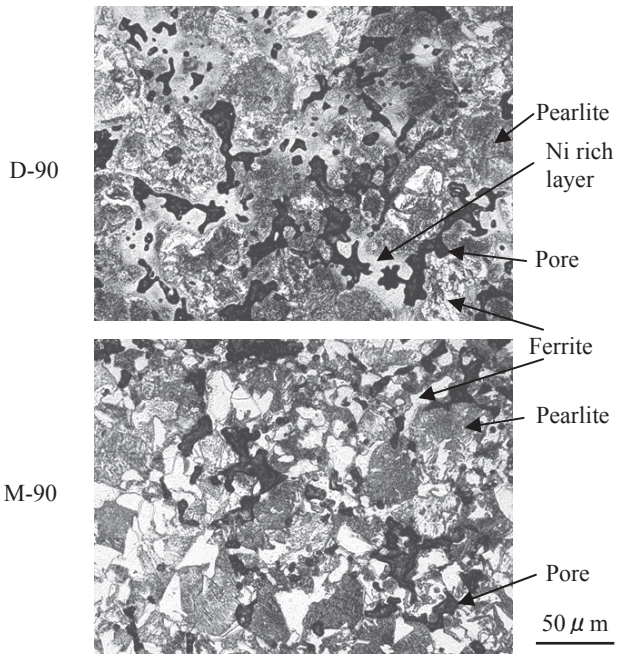

Fig.10 The microstructures of the Steel D and Steel M

4. Conclusions

A series of tensile experiments on conventional sintered steels, namely Fe-4Ni-1.5Cu-0.5Mo-0.5C (Steel D) and Fe-2Cu-0.5C (Steel M), were performed under low and high strain rates in this study. The results mainly obtained are summarised as follows:

(1) Larger tensile strengths were observed under high strain rates than under low strain rates in both the Steel D and M independently of relative density, however the difference of the strength was small.

(2) Tensile strength increased with increasing relative density in both the Steel D and M independently of strain rate.

(3) SEM observation revealed that the intergranular and transgranular fracture occurred in the Steel M and D, respectively, but no clear difference in such aspects between the quasi-static and impact tensile fracture was found.

Nomenclature

A cross sectional area of the Bars No.1 and No.2, m^2
A_S cross sectional area of the specimen, m^2
C_0 longitudinal elastic wave velocity of the Bars No.1 and No.2, m/s
E Young's modulus of the Bars No.1 and No.2, Pa
P_1 force at the Bar No.2/specimen interface, N
P_2 force at the Bar No.1/specimen interface, N
e nominal strain
$\dot{e}$ nominal strain rate, s^{-1}
l initial length of the specimen, m
s nominal stress, Pa
t time, s
ε true strain
$\dot{\varepsilon}$ true strain rate, s^{-1}
$\varepsilon_i(t)$ incident strain wave
$\varepsilon_t(t)$ transmitted strain wave
σ true stress, Pa

References

[1] JIS Z 2500 (2000), Powder Metallurgy -Vocabulary.
[2] Metal Powder Industries Federation: MPIF Standard 35, Materials Standards for PM Structural Parts, 2009 Edition (2009).

[3] ISO 5754 (1978), Sintered Metal Materials, Excluding Hardmetals -Unnotched Impact Test Piece.
[4] Degoix, C.N., Griffo, A. and German, R.M.: Effects of Sintering Parameters on the Mechanical Properties of a Fe-2Cu-2Ni-0.9Mo-0.8C Steel, *Int. J. Mater. Prod. Technol.*, **15**-3/5 (2000), 409-426.
[5] Degoix, C.N., Griffo, A. and German, R.M.: Effect of Lubtication Mode and Compaction Temperature on the Properties of Fe-Ni-Cu-Mo-C, *Int. J. Powder Metall.*, **34**-2 (1998), 29-33.
[6] Straffelini, G., Fontanari, V. and Molinari, A.: Comparison of Impact and Slow Bend Behavior of PM Ferrous Alloys, *Mater. Sci. Eng. A*, **A248**-1/2 (1998), 153-160.
[7] Straffelini, G., Fontanari, V. and Molinari, A.: Strain Hardening Behaviour of Sintered Steels under Tensile and Impact Loading, *Adv. Powder Metall. Part. Mater.*, **1994**-2 (1994), 51-59.
[8] Tremblay, L. and Chagnon, F.: Effect of Sintering Temperature and Time on Microstructure and Mechanical Properties of P/M Materials Made from Diffusion-bonded Powders, *Adv. Powder Metall. Part. Mater.*, **1997**-2 (1997), 13.53-13.65.
[9] Champagne, B., Angers, R. and Tremblay, S.: Mechanical Properties of Copper-infiltrated, Low-alloy P/M Steel and 316L P/M Stainless Steel, Prog. Powder Metall., **42**(1986), 373-390.
[10] Brewin, P.R., Nurthen, P.D., Davis, T. and Trilk, N.C.: The Effect of Cooling Rate and Carbon on Mechanical Properties in Ferrous Based Mixed Powder Systems, *Adv. Powder Metall. Part. Mater.*, **1994**-6 (1994), 187-198.
[11] Danninger, H.: Pore Formation during Sintering of Fe-Cu and its Effects on Mechanical Properties, *Powder Metall. Int.*, **19**-1 (1987), 19-23.
[12] O'Brien, R.C.: Impact and Fatigue Characterization of Selected Ferrous P/M Materials, *Prog. Powder Metall.*, **43** (1987), 749-775.
[13] Nahme, H., Lach, A.E. and Tarrant, A.: Mechanical Property Under High Dynamic Loading and Microstructure Evaluation of a TiB_2 Particle-reinforced Stainless Steel, *J. Mater. Sci.*, **44**-2 (2009), 463-468.
[14] Lee, W., Liu, T. and Lin, C.: Strain Rate Dependence of Impact Properties of Sintered 316L Stainless Steel, *J. Nucl. Mater.*, **359**-3 (2006), 247-257.
[15] Lee, W. and Chiu, C.: Deformation and Fracture Behavior of 316L Sintered Stainless Steel under Various Strain Rate and Relative Sintered Density Conditions, *Metall. Mater. Trans. A*, **37**-12 (2006), 3685-3696.
[16] Lee, W. and Chou, J.: The Effect of Strain Rate on the Impact Behaviour of Fe-2 mass% Ni Sintered Alloy, *Mater. Trans.*, **46**-4 (2005), 805-811.
[17] Engstrom, U.: Copper in P/M Steels, *Int. J. Powder Metall.*, **39**-4 (2003), 29-39.
[18] ISO 2740 (2009), Sintered Metal Materials, Excluding Hardmetals -Tensile Test Pieces.
[19] Nicholas, T., Tensile Testing of Materials at High Rates of Strain, *Exp. Mech.*, **21**-5 (1981), 177-185.